UBD modifies *APOL1*-induced kidney disease risk

Jia-Yue Zhang[a,b,1], Minxian Wang[a,b,1,2,3], Lei Tian[c], Giulio Genovese[d], Paul Yan[a,b], James G. Wilson[e], Ravi Thadhani[f,4], Amy K. Mottl[g], Gerald B. Appel[h], Alexander G. Bick[f,i], Matthew G. Sampson[j], Seth L. Alper[a,b,i], David J. Friedman[a,b], and Martin R. Pollak[a,b,i,2]

[a]Division of Nephrology, Department of Medicine, Beth Israel Deaconess Medical Center, Boston, MA 02215; [b]Department of Medicine, Harvard Medical School, Boston, MA 02115; [c]Stanford Cardiovascular Institute, Stanford University School of Medicine, Stanford, CA 94305; [d]Stanley Center for Psychiatric Research, Broad Institute of Harvard and Massachusetts Institute of Technology, Cambridge, MA 02142; [e]Department of Physiology and Biophysics, University of Mississippi Medical Center, Jackson, MS 39216; [f]Department of Medicine, Massachusetts General Hospital, Boston, MA 02114; [g]University of North Carolina Kidney Center, University of North Carolina School of Medicine, Chapel Hill, NC 27599; [h]Center for Glomerular Diseases, Columbia University Medical Center, New York, NY 10032; [i]Broad Institute of Harvard and Massachusetts Institute of Technology, Cambridge, MA 02142; and [j]Department of Pediatrics, University of Michigan School of Medicine, Ann Arbor, MI 48109

Contributed by Martin R. Pollak, January 28, 2018 (sent for review September 22, 2017; reviewed by Ali Gharavi and Susan E. Quaggin)

People of recent African ancestry develop kidney disease at much higher rates than most other groups. Two specific coding variants in the Apolipoprotein-L1 gene *APOL1* termed G1 and G2 are the causal drivers of much of this difference in risk, following a recessive pattern of inheritance. However, most individuals with a high-risk *APOL1* genotype do not develop overt kidney disease, prompting interest in identifying those factors that interact with *APOL1*. We performed an admixture mapping study to identify genetic modifiers of *APOL1*-associated kidney disease. Individuals with two *APOL1* risk alleles and focal segmental glomerulosclerosis (FSGS) have significantly increased African ancestry at the *UBD* (also known as FAT10) locus. UBD is a ubiquitin-like protein modifier that targets proteins for proteasomal degradation. African ancestry at the *UBD* locus correlates with lower levels of *UBD* expression. In cell-based experiments, the disease-associated *APOL1* alleles (known as G1 and G2) lead to increased abundance of *UBD* mRNA but to decreased levels of *UBD* protein. *UBD* gene expression inversely correlates with G1 and G2 *APOL1*-mediated cell toxicity, as well as with levels of G1 and G2 APOL1 protein in cells. These studies support a model whereby inflammatory stimuli up-regulate both *UBD* and *APOL1*, which interact in a functionally important manner. UBD appears to mitigate *APOL1*-mediated toxicity by targeting it for destruction. Thus, genetically encoded differences in *UBD* and *UBD* expression appear to modify the *APOL1*-associated kidney phenotype.

APOL1 | *UBD* | FAT10 | kidney | FSGS

Kidney disease is much more common in people of recent African ancestry than in other groups. Two coding variants in the *APOL1* gene are the drivers of much of this difference in disease risk (1, 2). The more common of these alleles, G1, encodes two amino acid substitutions near the C terminus of the protein that almost always occur together. The second risk allele, G2, is a two-amino acid deletion adjacent to the location of the G1 allele. Two risk alleles are required for these large increases in risk, consistent with a recessive mode of inheritance.

It is remarkable that variants as common as *APOL1* G1 and G2 have such a large effect on the risk of multiple forms of kidney disease. The increased risk in individuals compound heterozygous or homozygous for *APOL1* risk alleles is approximately fourfold to sevenfold for hypertension-associated end-stage renal disease (H-ESRD), 17-fold for FSGS, and 29- to 89-fold for HIV-associated nephropathy (3, 4). The mechanism(s) of *APOL1*-associated kidney disease risk remain unclear. However, investigators have consistently shown, in cell culture and in vivo systems, that the high-risk *APOL1* variants are toxic to cells (reviewed in ref. 5).

Despite the high risk of kidney disease associated with *APOL1*, most people with a high-risk *APOL1* genotype neither have nor develop kidney disease. Our rough estimates put the lifetime risk of nondiabetic ESRD and/or chronic kidney disease (CKD)-related mortality in people with a high-risk genotype at about 20%, in contrast to 2% to those without. This raises obvious questions: Why do some people with the high-risk genotype develop kidney disease but not others? Why do some develop early-onset FSGS and others late-onset progressive CKD and ESRD? Both genetic and nongenetic factors likely can modify the clinical phenotype associated with a high-risk *APOL1* genotype, leading to various forms of overt kidney disease (and/or protecting against overt kidney disease) in some but not others.

Here we show that variation at the *UBD* locus (also called *FAT10*) is a genetic modifier of the risk of FSGS in individuals with a high-risk *APOL1* genotype. *UBD* encodes a ubiquitin-like protein modifier that targets proteins to the 26S proteasome for degradation (6, 7). Like *APOL1*, *UBD* is up-regulated in response to proinflammatory stimuli including IFN-γ (8). In a mouse model of HIV-associated nephropathy, *UBD* is among the most up-regulated genes in the kidney (9). Previous studies have shown that intrarenal

Significance

Two common variants in the *APOL1* gene explain most of the high rate of kidney disease in people of recent African ancestry. However, not all *APOL1* high-risk individuals develop kidney disease. Here we identified the *UBD* locus as a genetic modifier of *APOL1* kidney disease using admixture mapping. Focal segmental glomerulosclerosis patients have significantly increased African ancestry at the *UBD* locus, which associates with lower *UBD* gene expression. Using a cell-based system, we show that UBD and APOL1 interact functionally and that higher levels of *UBD* expression mitigate *APOL1*-mediated cell death. These findings are important for understanding the genetic and functional modifiers of the human *APOL1*-associated phenotype and the biological pathways relevant to *APOL1*-associated cell damage.

Author contributions: J.-Y.Z., M.W., M.G.S., S.L.A., D.J.F., and M.R.P. designed research; J.-Y.Z., M.W., P.Y., and J.G.W. performed research; J.G.W., R.T., A.K.M., and G.B.A. contributed new reagents/analytic tools; J.-Y.Z., M.W., L.T., G.G., A.G.B., S.L.A., D.J.F., and M.R.P. analyzed data; and J.-Y.Z., M.W., D.J.F., and M.R.P. wrote the paper.

Reviewers: A.G., Columbia University; and S.E.Q., Feinberg School of Medicine, Northwestern University.

Conflict of interest statement: M.R.P. and S.E.Q. are coauthors on a 2014 review article. M.G.S. and G.B.A. are coauthors on several papers published in the past 4 years with A.G. D.J.F. and M.R.P. have filed patents related to ApoL1-associated kidney disease and own equity in ApoLo1 Bio, LLC.

Data deposition: Data used in this study have been deposited on figshare (https://doi.org/10.6084/m9.figshare.5917771).

[1]J.-Y.Z. and M.W. contributed equally to this work.

[2]To whom correspondence may be addressed. Email: minxian@broadinstitute.org or mpollak@bidmc.harvard.edu.

[3]Present address: Program in Medical and Population Genetics, Broad Institute of Harvard and Massachusetts Institute of Technology, Cambridge, MA 02142.

[4]Present address: Department of Biomedical Sciences, Cedars Sinai Medical Center, Los Angeles, CA 90048.

This article contains supporting information online at www.pnas.org/lookup/suppl/doi:10.1073/pnas.1716113115/-/DCSupplemental.

Published online March 12, 2018.

expression of *UBD* is increased in individuals with glomerular disease and a high-risk *APOL1* genotype (10).

By use of admixture mapping, we demonstrate that individuals with a high-risk *APOL1* genotype and FSGS have significantly increased African ancestry at the *UBD* locus compared with their whole genome background and compared with control groups at this locus. African ancestry at the *UBD* locus is associated with lower levels of *UBD* RNA expression. Using cell-based experiments, we demonstrate that UBD interacts with APOL1 to modify *APOL1* risk variant-mediated cell death. Specifically, we show that induction of expression of the toxic variant forms of *APOL1* in a cell system leads to increased expression of *UBD* mRNA. Increased expression of *UBD* leads to a decrease in the amount of the G1 and G2 APOL1 protein (but not the nondisease-associated G0 form).

Results

Detecting Ancestral Biases for FSGS in Individuals with High-Risk *APOL1* Genotypes. We genotyped DNA from 253 African American (AA) individuals with either FSGS or nondiabetic ESRD to identify potential loci that interact with and modify the *APOL1*-associated phenotype(s). We used admixture mapping to discover genetic modifier(s) for the *APOL1* high-risk genotype individuals (G1G1, G2G2, or G1G2) with FSGS, then compared the candidate loci with *APOL1* high-risk individuals with ESRD and high-risk people without known kidney disease, conditioned on each person's genome-wide admixture background. We also compared the genome-wide ancestries between different groups. We replicated our findings by genotyping an additional 62 FSGS samples (Fig. S1 and Table S1).

We examined FSGS as our primary phenotype of interest. Although most forms of nondiabetic CKD are associated with the *APOL1* risk genotype, risk is much stronger with FSGS, a histologically defined (and presumably a more uniform) phenotype. We developed a ranked list of genomic loci, ordered by the degree of ancestry bias. We ranked loci by the number of SDs above (African ancestry enriched) or below (European ancestry enriched) the average African ancestry. For each SNP in the genome, we also applied a log likelihood ratio test (11) by comparing the disease-associated model with the null model to estimate the ancestry disease risk.

For admixture mapping, local ancestry was inferred by RFMix (12) and HAPMIX (13) programs. Both methods use data from ancestral populations (here African and European) as references to train a statistical model and then estimate the most likely ancestry states of the sequence of each query sample. We used the phased sequencing data of 99 YRI and 99 CEU from 1000 Genomes Project Phase 3 (14) as reference for RFMix. We also used the genotyping data of 113 YRI and 112 CEU individuals from HapMap (15) as reference for HAPMIX to replicate the ancestry inferring process. As the results of them were highly concordant, we present the results obtained using RFMix in this paper (Fig. S2).

For each individual, after local ancestry inference, we determined genome-wide ancestry and local ancestry at loci throughout the genome. The *APOL1* high-risk genotype individuals studied included individuals with FSGS, AA individuals with ESRD, AA individuals from the Jackson Heart Study with or without CKD, and high-risk individuals imputed from two collections of samples available through the dbGAP database without kidney phenotype information but genotyped using the same platform as we used for the FSGS discovery and ESRD groups (phs000507 and phs000560) (Table S1).

We first compared the overall percentage of European and African ancestry in these different sample sets. Individuals with a high-risk *APOL1* genotype had similar fractions of recent European ancestry except for the FSGS groups. The FSGS groups exhibited markedly higher proportions of recent European ancestry, despite sharing the high-risk *APOL1* genotype, which is exceedingly rare except in people self-identified as AA. This difference (Fig. 1*A*) may reflect the methods of ascertainment and sample selection rather than any underlying biology as members of this FSGS cohort were chosen on the basis of *APOL1* genotype, whereas self-identified AA race was a prerequisite for entry into the other study groups.

We then estimated the locus-specific African ancestry for each group after normalizing global ancestry person by person, following the method in Patterson et al. (16) to control the global ancestry difference between study groups. Using two complementary local ancestry inference algorithms and two sources of reference data (12, 13), we sought loci with ancestral bias greater than 3 SDs from

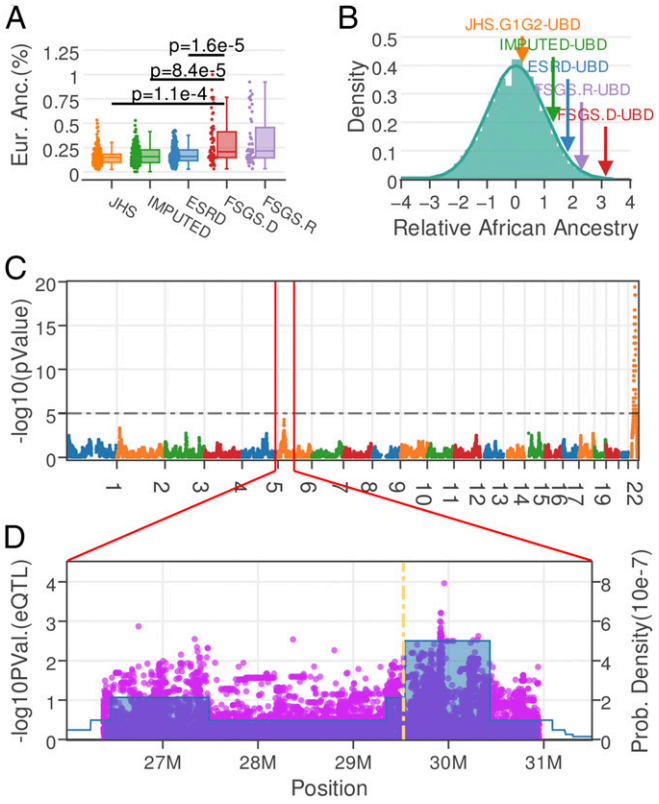

Fig. 1. Admixture mapping and locus fine mapping. (*A*) Comparison of admixture in the different groups studied. The percentage of European (CEU) and sub-Saharan African (YRI) ancestry was compared. Individuals with a high-risk *APOL1* genotype had similar fractions of recent African ancestry with the exception of the FSGS group, which exhibited markedly greater recent European ancestry despite sharing a high-risk *APOL1* genotype with all groups. FSGS.D represents the FSGS discovery group, and FSGS.R represents the FSGS replication group. Significance was evaluated by *t* test. (*B*) Ancestral bias at the *UBD* locus for the different groups studied. At any locus, the ancestry deviating from a normalized relative African ancestry of 0 was estimated. Positive values indicate enrichment of African ancestry, whereas negative values indicate enrichment of European ancestry. The *UBD* locus shows the largest bias toward enrichment of African ancestry in the FSGS discovery and replicate group. The histogram bar distribution was estimated from empirical data, and the curved line was fitted as a normal distribution against empirical data. FSGS.D represents the FSGS discovery group, and FSGS.R represents the FSGS replication group. (*C*) Admixture mapping across the whole genome for FSGS high-risk genotype individuals. *P* value was estimated by a likelihood ratio test method that determines ancestral bias at each locus, conditioned on each individual's global ancestry. The data from FSGS discovery and replication group were combined together for this estimation. (*D*) Fine mapping for causal variants and *UBD* eQTL around the *UBD* locus. The blue curve shows the relative probability where the causal variants are located based on the degree of ancestry bias. The blue shaded area is the 95% credible interval from the central area under the curve peak, from 26,378,681 to 30,951,367 bp (hg19), containing 148 genes. The area under the entire curve was normalized as 1. Purple dots denote the *P* value for each SNP considered as an eQTL for *UBD*. The most likely causal locus coincides with the most significant eQTLs of the *UBD* gene. The vertical yellow dashed line indicates the location of the *UBD* gene. There are no *UBD* transcripts directly overlapping with the most ancestry-biased region.

Table 1. Ancestry bias at *UBD* locus

Group	FSGS	ESRD	dbGAP	JHS
Genome-wide average*	69.4% (148)	82.5% (282)	83.0% (360)	84.6% (504)
UBD locus†	79.9% (171)	86.8% (297)	85.3% (370)	84.6% (504)
Total haplotypes	214	342	434	596
Odds ratio (95% CI)	1.77 (1.11–2.84)	1.40 (0.90–2.19)	1.19 (0.81–1.74)	1 (0.72–1.39)

Comparison of local ancestry at the *UBD* locus with genome-wide average of different *APOL1* high-risk genotype groups. For the FSGS group, 59 discovery and 48 replication individuals were combined for this estimate, for a total of 214 haplotypes. The number in parentheses is the number of haplotypes. The ancestry bias odds ratio is 1.77 per *UBD* haplotype in the FSGS group, or 1.42 if estimated by the maximum likelihood method, multiplicative model.

*Estimated by the genome-wide average ancestry proportion times the total number of haplotypes.

†Directly counted through the ancestry label estimated by RFMix software at *UBD*.

the mean relative African ancestry in the FSGS group. We illustrate this approach by plotting the results for the Chr6p21.33–22.2 locus that we term the *UBD* locus (Fig. 1*B*). This locus has African ancestry 3.2 SDs beyond the mean in the discovery group and 2.3 SDs in replication group.

Other than the *APOL1* locus itself on Chr22, only two loci reached the 3 SD threshold: Chr6p21.33–22.2 (Table 1) and Chr18q22.3–23 in the discovery group. The deviation at the Chr6 locus was replicated in a second smaller FSGS group (Fig. 1*B* and Fig. S2), whereas the locus on Chr18 did not replicate. For the Chr6 locus, a P value $= 4.8 \times 10^{-5}$ [false discovery rate (FDR) = 0.0061] representing the African ancestry bias was obtained using the combined data from the FSGS groups. Despite having more European ancestry at a genome-wide level, the high-risk *APOL1* FSGS individuals were nevertheless enriched for African ancestry at the chromosome 6 locus (Fig. 1 and Fig. S1). Thus, we prioritized this locus for further evaluation.

Fine Mapping at the Chr6 Locus. We performed fine mapping in an effort to isolate causal variants and genes at the Chr6 locus. Based on the log likelihood ratio score estimated by Eq. **S1** (ADM test), which maximizes the likelihood for estimation of ancestry disease risk, we estimated the relative probability of each SNP (or its highly linked sites) within the Chr6p locus as being causal, and also the 95% confidence interval for the causal allele of this locus (Fig. 1*D*), following the method of Freedman et al. (17). The 95% confidence interval is located from 26,378,681 to 30,951,367 bp (hg19), containing 148 genes. The most ancestry-biased region is located from 29,543,646 to 30,434,900 bp (hg19) and referred to as the high-risk region hereafter.

G1 and G2 both originated recently (18). We hypothesized that variability in the *APOL1* associated phenotype may be influenced by differences in expression of modifier genes because most GWAS loci are located in regulatory regions (19, 20). By using the data from the Genetic European Variation in Health and Disease, A European Medical Sequencing Consortium (GEUVADIS) Project (21) and normalizing the RNA sequencing data to control for confounding factors (22, 23), we first checked for genes with cis-eQTL peaks (FDR ≤ 0.2) located in this high-risk region, where the peak was defined as the most significant SNP that correlated with gene expression. The eQTLs were estimated using data available from the YRI population to determine the effect of African ancestry at the Chr6p locus. There are 33 genes that meet this criterion. We compared the population-level gene expression for these genes between YRI and CEU populations (t test), as we hypothesized that gene expression difference was the driving force for ancestry bias at this locus. Only two genes meet both criteria, *UBD* and *PPP1R18* (FDR < 0.2 for expression difference). We focused our attention on the *UBD* gene because *UBD* is among the three most highly up-regulated genes in glomeruli from nephrotic syndrome patients with a high-risk *APOL1* genotype compared with other genotypes (10). The most highly associated SNPs in this region overlap with the SNPs that represent the strongest eQTLs for *UBD* (Fig. 1 and Table S2). As shown in Fig. 2, the YRI individuals have, on average, significantly lower *UBD* expression than those from the CEU population (P value $= 8.4 \times 10^{-4}$, FDR = 0.015). Taken together, this implies that higher African ancestry at this locus is associated with lower levels of *UBD* expression and prompted us to test the effect of *UBD* expression on *APOL1* in a cell-based system.

We note that there are coding variants in *UBD*. Combinations of these variants form haplotypes with different frequencies in Africans and Europeans. However, these coding variants are not located in the region that shows the greatest ancestry bias in the FSGS samples. (We also performed functional testing of the major haplotypes defined by these variants between the YRI and CEU populations and saw no difference in the effect of these haplotypes on *APOL1*-associated cell toxicity as below.)

Expression of *APOL1* Risk Variants Leads to Up-Regulation of *UBD* Transcript but Reduces Endogenous *UBD* Protein Level. *UBD* is a ubiquitin-like protein modifier (6). Both *UBD* and *APOL1* are up-regulated in response to inflammatory stimuli and may play roles in the innate immune system (10, 24, 25). Sampson et al. (10) showed that *UBD* is among the three most up-regulated genes in glomeruli from nephrotic syndrome patients with a high-risk *APOL1* genotype. We therefore explored this interaction further using cellular assays.

We previously generated T-REx-293 stable cell lines that express Flag-tagged *APOL1* G0, G1, and G2 isoforms under the control of tetracycline (tet) (26). An empty vector (EV) control cell line contains only the plasmid backbone. Induction of G1 and G2 expression (but not G0) leads to a marked increase in *UBD* mRNA (Fig. 3). In contrast to *UBD* mRNA, endogenous *UBD* protein level was reduced in G1- and G2-expressing cells compared with untreated cells and

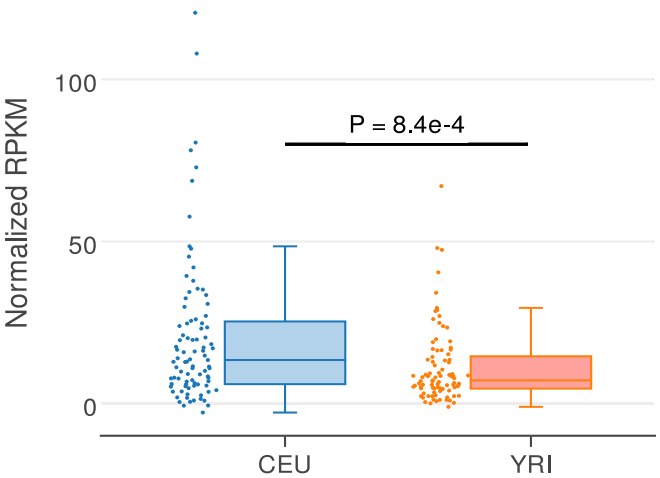

Fig. 2. *UBD* gene expression in CEU and YRI populations. Each dot represents an individual's *UBD* gene expression (in EBV-transformed lymphoblastoid cell lines) measured by PEER method normalized reads per kilobase per million (RPKM) mapped reads (23). Significance was evaluated by t test.

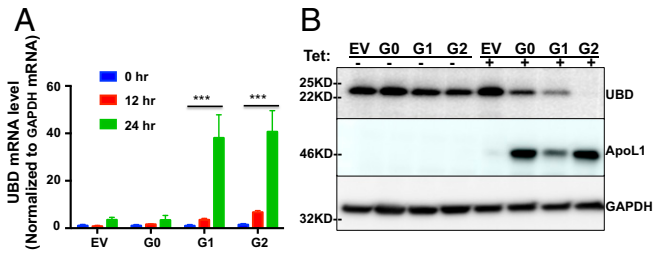

Fig. 3. Induction of *APOL1* G1 and G2 leads to up-regulation of *UBD* transcripts but reduced UBD protein levels. (*A*) Quantitative PCR of *UBD* and GAPDH transcripts after *APOL1* induction in T-REx-293 cells with tet (50 ng/mL; eight replicates). (*B*) Immunoblot of *UBD*, *APOL1*, and GAPDH after induction with tet (50 ng/mL) for 24 h; four replicates. ***$P < 0.01$. Significance was evaluated by *t* test. Error bar represents SD.

G0 cells (Fig. 3*B*). For comparison, we quantified the transcript level of the ubiquitin gene UBB as well as the *GABBR1* gene that overlaps in genomic location with *UBD*. The induction of *APOL1* expression did not affect the mRNA level of either *UBB* or *GABBR1* (Fig. S3).

***UBD* Overexpression Decreases *APOL1* Risk Variants-Induced Cytotoxicity.** Previous studies noted that *UBD* overexpression (27–29) may lead to apoptosis. We transiently transfected the *APOL1* T-REx-293 stable cell lines with *UBD* (pCMV6-*UBD*-HA) or EV control (pCMV6-entry) for 24 h followed by 24 h tet induction of *APOL1*. The cytotoxicity/viability ratio decreased significantly in G1 and G2 cell lines in the presence of *UBD*-HA overexpression (Fig. 4*A*). To confirm whether the cytotoxicity/viability ratio correlated with *UBD* expression, we transiently transfected different amounts of pCMV6-*UBD*-HA plasmid, balanced by EV plasmid to keep constant the total amount of transfected cDNA. As the UBD protein level increased, *APOL1*-associated cytotoxicity in G1 and G2 cell decreased (Fig. 4). This relationship was not observed in EV or G0 cell lines.

Inactivation of *UBD* by siRNA and CRISPR Leads to Increased *APOL1*-Induced Cytotoxicity. To investigate the association between the dose of *UBD* and *APOL1*-induced cytotoxicity, we inactivated endogenous *UBD* via both siRNA and CRISPR. For knockdown of *UBD* by siRNA, we transiently transfected T-REx-293 cells either with siUBD or with control siRNA and allowed the cells to grow for 48 h. In G1- and G2-expressing *UBD* knockdown cells, but not in cells treated with control siRNA, there was a substantial increase in *APOL1* G1- and G2-mediated cytotoxicity (Fig. 4*D*). Previous studies have shown that in HeLa cells, knockdown of *UBD* by siRNA leads to cell death (30). However, here we did not find any significant changes in cytotoxicity in EV and G0 knockdown cells. We note that the observed change in cytotoxicity did not require particularly high knockdown efficiency (53%).

For *UBD* gene inactivation by CRISPR, we infected the T-REx-293 cells with virus and appropriate sgRNAs and controls and then selected single colonies. Immunoblots were done to identify cell colonies in which *UBD* was inactivated (Fig. 4*F*). In *UBD*-inactivated cells, G1- and G2-induced cytotoxicity became severe within 18 h of tet induction of *APOL1* (Fig. 4*E*), more than with siRNA knockdown, consistent with more complete *UBD* inactivation by CRISPR. In the EV and G0 cells, *UBD* inactivation did not alter cytotoxicity.

***UBD* Overexpression Leads to Decreased *APOL1* G1 and G2 Protein but Not G0.** To test whether *UBD* overexpression altered *APOL1* levels in T-REx-293 stable cell lines, we immunoblotted whole-cell lysates prepared after transient transfection with *UBD* (pCMV6-*UBD*-HA), which overexpresses UBD with a hemagglutinin (HA) tag, or empty vector as a control, followed by tet induction for 24 h. Even with high levels of *APOL1* induction in the stable cell lines, *UBD* expression led to a clear decrease in G1 and G2 protein but no noticeable change in G0 protein (Fig. 5*A*). Immunoblotting with anti-HA showed that UBD protein level is much lower in *APOL1* G1- and G2-expressing cells compared with G0 cells, consistent with the results of endogenous UBD protein level (Fig. 3*B*). This suggests increased degradation of both APOL1 and UBD. We performed RT-PCR to see if *UBD* overexpression affects APOL1 protein level directly or rather influences *APOL1* RNA level. *UBD* overexpression had no effect on the mRNA level of *APOL1* (Fig. 5*B*).

***UBD* Interacts with *APOL1*.** These results imply that UBD interacts with APOL1 and targets it for degradation in the presence of G1 or G2 alleles. To confirm an interaction between UBD and APOL1 in vivo and the effect of proteasome inhibition on any such interaction, we performed coimmunoprecipitation (co-IP) experiments. T-REx-293 cells were tet-induced (50 ng/mL) for 9 h, with or without proteasome inhibitor MG132 (or DMSO as negative control) during the final 4 h. Lysates were subjected to IP with anti-*FLAG* (APOL1) and immunoblotted with anti-*UBD*. The interaction between UBD and each APOL1 variant was more easily detected with proteasome inhibition (Fig. 6). To confirm the interaction of APOL1 and UBD, we performed bidirectional co-IP. We observed that the G0, G1, and G2 forms of APOL1 all coimmunoprecipitated with anti-UBD. Endogenous UBD protein was detectable by APOL1 IP as well.

Discussion

In this study, we demonstrate that individuals with FSGS and a high-risk *APOL1* genotype are enriched for recent African ancestry at the *UBD* locus. The moderate number of *APOL1* high-risk

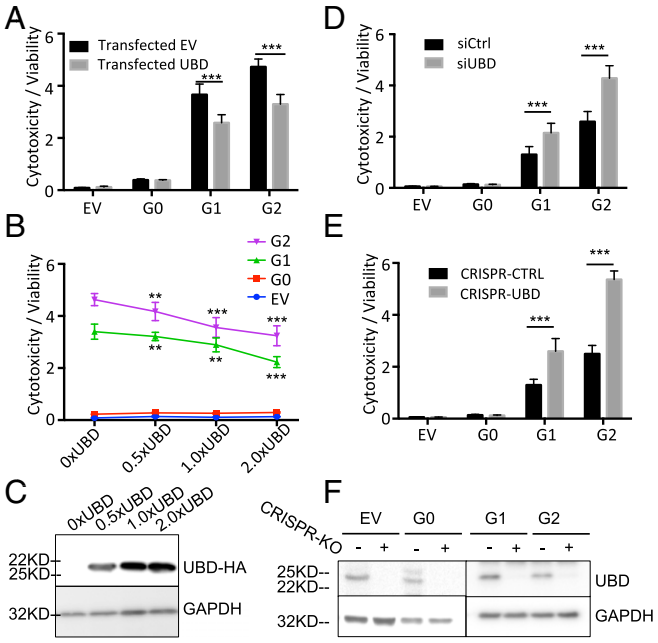

Fig. 4. *UBD* expression level alters *APOL1* G1- and G2-induced cytotoxicity. *UBD* overexpression reduces *APOL1* G1- and G2-induced cytotoxicity, whereas inactivation of *UBD* by siRNA and CRISPR leads to increased *APOL1*-induced cytotoxicity. (*A*) Cell cytotoxicity/viability after 24-h treatment with tet (50 ng/mL) in the presence or absence of transiently transfected *UBD* for an additional 24 h. (*B*) Cell cytotoxicity/viability after 24 h tet (50 ng/mL) treatment with transiently transfected *UBD* cDNA for an additional 24 h. (*C*) Immunoblot of overexpressed UBD-HA after transfection with the indicated relative amounts of *UBD* cDNA. (*D*) Cell cytotoxicity/viability after 24 h posttransfection with or without *UBD* siRNA (siRNA or siCTRL) followed by 18 h tet induction (50 ng/mL) of the induced *APOL1* variants. (*E*) Cell cytotoxicity/viability of the indicated *APOL1* cell lines (with or without CRISPR inactivation of *UBD*) after 18 h tet (50 ng/mL) induction. (*F*) Immunoblot of endogenous UBD in the induced cell lines with (+) or without (–) CRISPR inactivation of *UBD*. (In *A*, *B*, *D*, and *E*, **$P < 0.05$, ***$P < 0.01$ vs. untreated cells, eight replicates.) Significance was evaluated by *t* test. Error bar represents SD.

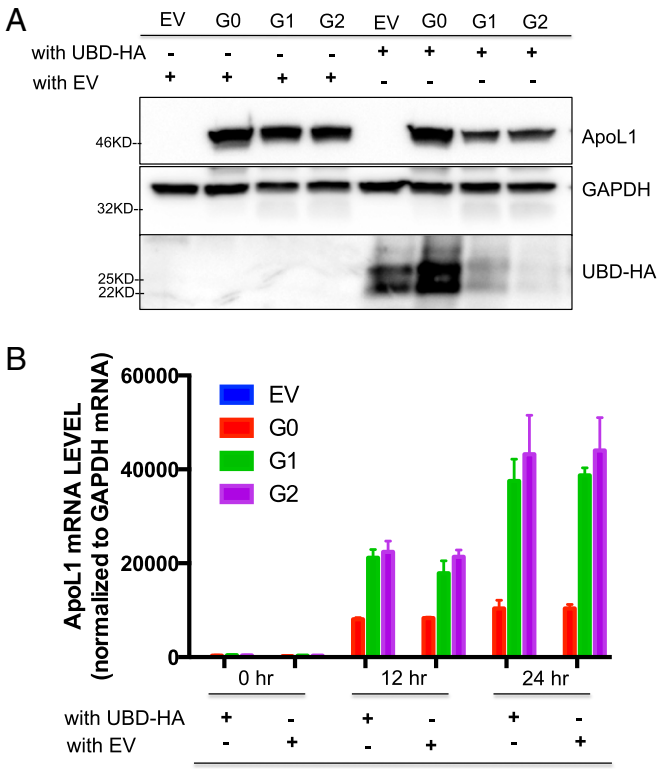

Fig. 5. *UBD* overexpression leads to decreased expression of G1 and G2 *APOL1* protein. (*A*) Immunoblot of *APOL1*, *UBD*-HA, and GAPDH in T-REx-293 cells 24 h after transfection with or without *UBD*-HA cDNA followed by tet (50 ng/mL) induction of the indicated *APOL1* variants for another 24 h. *UBD* overexpression leads to decreased expression of G1 and G2 *APOL1* protein without apparent change of G0 protein. (*B*) Quantitative PCR of *APOL1* (normalized to GAPDH) in the presence or absence of *UBD*-HA overexpression and subsequent tet induction of *APOL1*. *UBD*-HA overexpression has no effect on *APOL1* transcripts (four replicates).

genotype FSGS samples available made admixture mapping a more robust approach than standard GWAS. GWAS tests association on a SNP by SNP basis, whereas admixture mapping tests for association based on ancestry block, greatly decreasing the multiple testing correction burden. The key comparison in a study such as this is the relative amount of African (or European) ancestry at specific regions of the genome compared with the genome as a whole. Here the strongest admixture signal we found at Chr6p overlaps precisely with the strongest *UBD* eQTLs. Expression of this gene is significantly different between people of African and European ancestry, making differential *UBD* expression the likely driver of this ancestry bias.

Although we were able to localize an FSGS-modifying region (a 95% credible interval), we do not have enough power to pinpoint the causal position and SNP(s). We note that several HLA genes are located in the high-risk region within the Chr6p locus. Under the assumption that ancestry-dependent risk at this locus is driven by alterations in gene expression, we can exclude the HLA genes because they do not show significant expression differences between Africans and Europeans. However, ancestry-associated differences in *UBD* gene expression may also reflect a genetic hitchhiker effect (31), driven by sequence differences in nearby HLA genes or other genes. Together with the biological validation in this study as well as previous observations regarding *UBD* expression (10, 32–34), there is strong support for the notion that the *UBD* gene plays a critical role in the regulation of *APOL1*-induced disease risk and that ancestry bias at this locus is associated with increased risk of FSGS in the setting of a high-risk *APOL1* genotype. Nevertheless, we cannot definitely exclude HLA genes as possible contributors. Further studies of larger populations of *APOL1*-associated FSGS may be able to better define the specific SNPs that are driving ancestry bias and in addition influencing the risk of FSGS. We note that our functional studies showed that coding differences in the major haplotypes of African and European populations do not explain *UBD*'s effect on *APOL1*-associated cell death, which is consistent with *UBD* expression rather than *UBD* coding sequence itself as responsible for differences in *APOL1*-associated FSGS.

UBD is an interesting gene for several reasons. HIV is the strongest known nongenetic hit for the development of kidney disease in the setting of a high-risk *APOL1* genotype. *UBD* is among the most highly up-regulated genes in HIV-infected cells (34). Both *UBD* and *APOL1* are up-regulated in response to inflammatory stimuli and may play roles in the innate immune system (10, 24, 25). Using an unbiased approach, Sampson et al. (10) showed that *UBD* is among the three most up-regulated genes in glomeruli from nephrotic syndrome patients with a high-risk *APOL1* genotype. A mouse model of *APOL1*-associated disease showed a similar change in *UBD* expression (32). A genome-wide study of circulating *APOL1* levels pointed toward *UBD* (or a locus near *UBD*) as an expression QTL for *APOL1* (33). Thus, genetic, transcriptional, and functional data all intersect at the *UBD* locus, strongly suggesting that it may play a role in modulating the effect of *APOL1* variants on the kidney. The present study suggests that ancestry-dependent variation at *UBD* itself modifies the risk of *APOL1*-associated FSGS. Furthermore, we show that at a cellular level, UBD and APOL1 interact as assessed by coimmunoprecipitation and functional effects on *APOL1*-mediated cell death. The previous observation that *UBD*

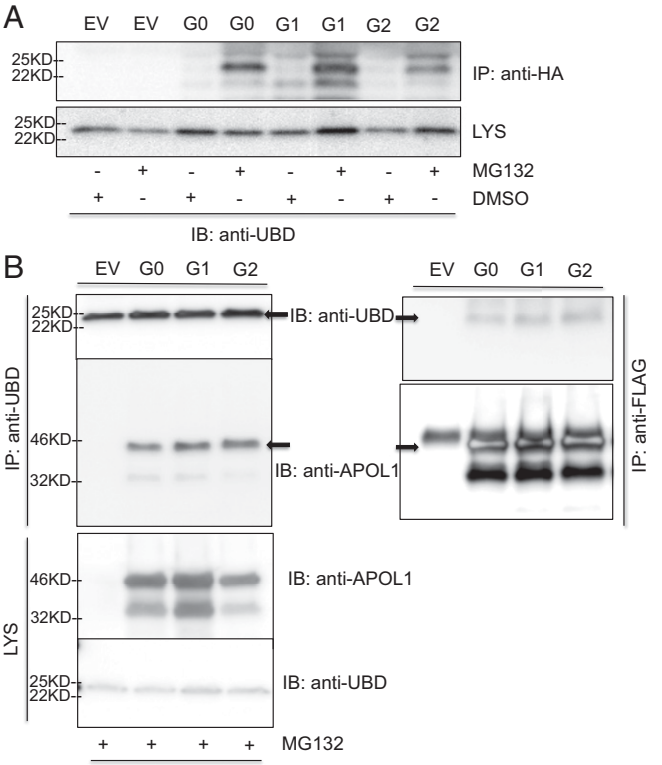

Fig. 6. *APOL1* and *UBD* interact. (*A*) T-REx-293 cells were tet-induced for 9 h, with or without 5 μM MG132 added during the final 4 h. Cells were then lysed and subjected to immunoprecipitation (IP) by anti-FLAG (*APOL1*) antibody, then immunoblotted with anti-*UBD* antibody. (*B*) The same experiment performed in the presence of MG132, and immunoprecipitation (IP) by anti-FLAG (*APOL1*) or anti-*UBD* antibody, followed by immunoblotting with anti-*UBD* or anti-*APOL1* antibody as indicated. The interaction between *APOL1* and endogenous *UBD* is more easily detected in the presence of proteasome inhibition.

is up-regulated in the kidney in the setting of *APOL1*-associated glomerular disease, together with the observations presented here, suggests that intrarenal *UBD* up-regulation may limit renal injury caused by up-regulation of *APOL1* (10, 32).

UBD encodes a ubiquitin-like protein that modifies and targets proteins for degradation via the 26S proteasome (6). Using a cell-based system, we show that expression of the disease-associated G1 and G2 forms of *APOL1*, but not G0, leads to marked up-regulation of the *UBD* transcript. By contrast, less UBD protein (endogenous or overexpressed) is detectable in this setting. Additionally, overexpression of *UBD* leads to a decrease in the amount of G1 and G2 APOL1 (but not G0) protein that is detectable in cells. G0, G1, and G2 all co-IP with UBD, and this interaction is more easily detected when the proteasome is inhibited. In the cell system used here, the G1 and G2 forms of *APOL1* led to marked up-regulation of *UBD* transcript not seen with the G0 form. In contrast to RNA, UBD protein is lower in G1 and G2 cells, suggesting much more rapid turnover of the *UBD* protein in the presence of G1 or G2 than with G0. Both the genetic and cellular data suggest that *UBD* may mitigate the toxic effects of G1 and G2. In proinflammatory states where both *UBD* and *APOL1* are up-regulated, this may be particularly relevant. The association of FSGS with *UBD* eQTLs is consistent with the model that UBD interacts with disease-associated G1 and G2 forms of APOL1 and targets it for proteasomal degradation, partially reducing its toxic effects (Fig. S4).

In vivo, lower levels of *UBD* may lead to reduced protection from *APOL1*-mediated toxicity, consistent with the observed effects of *UBD* on *APOL1*-mediated cell toxicity. *UBD* SNPs that are associated with lower level of *UBD* expression (as, on average, is seen in Africans compared with Europeans) are associated with higher FSGS risk. The opposite effects of *UBD* knockdown versus overexpression on cytotoxicity support this notion. UBD can modify proteins covalently or noncovalently (35). The lack of UBD-dependent changes in apparent M_r of APOL1 as assessed by denaturing gel electrophoresis suggests that UBD does not covalently modify APOL1.

The observations reported here raise several questions. Larger-scale human genetic studies may be able to further pinpoint specific variants that control *UBD* expression and in turn modify the *APOL1*-associated kidney phenotype. Further elaboration of the UBD–APOL1 interaction in in vivo models could provide insights into approaches to mitigate *APOL1*-associated kidney disease for therapeutic benefit. Although we observe effects of UBD in the context of APOL1, UBD may have a more general role in the degradation of cytotoxic proteins in glomerular as well as non-glomerular renal cells. Altered expression of *UBD* in other models supports this notion (25, 34). In the case of humans, and in a mouse model of *APOL1*-associated disease, up-regulation of *UBD* was observed in glomerular cells (10, 32). The natural experiment reported here suggests at least one potential therapeutic opportunity for treatment of *APOL1*-associated disease: factors that modulate the turnover of *APOL1* may represent a possible avenue for therapeutic intervention.

Materials and Methods

The human genetics studies were approved by the institutional review board (IRB) at Beth Israel Deaconess Medical Center. FSGS cases were ascertained following informed consent as part of a study of FSGS genetics ongoing since 1996. Other genetic datasets were obtained through dbGAP and the Jackson Heart Study. Detailed description of admixture mapping and other genetic methodologies used are described in *SI Materials and Methods*. Biochemical and cell-based assays were performed following standard procedures as described in *SI Materials and Methods*.

ACKNOWLEDGMENTS. The authors thank the staff and participants of the Jackson Heart Study (JHS). This work is supported by NIH Grants MD007092, MD007898, DK54931, and U54GM115428; US Department of Defense Grant W81XWH-14-1-0333; grants from the Ellison and Nephcure Foundations, and Vertex Pharmaceuticals. The JHS is supported and conducted in collaboration with Jackson State University (Grants HHSN268201300049C and HHSN268201300050C), Tougaloo College (Grant HHSN268201300048C), and the University of Mississippi Medical Center (Grants HHSN268201300046C and HHSN268201300047C) contracts from National Heart Lung Blood Institute and National Institute on Minority Health and Health Disparities.

1. Genovese G, et al. (2010) Association of trypanolytic ApoL1 variants with kidney disease in African Americans. *Science* 329:841–845.
2. Tzur S, et al. (2010) Missense mutations in the APOL1 gene are highly associated with end stage kidney disease risk previously attributed to the MYH9 gene. *Hum Genet* 128:345–350.
3. Kopp JB, et al. (2011) APOL1 genetic variants in focal segmental glomerulosclerosis and HIV-associated nephropathy. *J Am Soc Nephrol* 22:2129–2137.
4. Kasembeli AN, et al. (2015) APOL1 risk variants are strongly associated with HIV-associated nephropathy in black South Africans. *J Am Soc Nephrol* 26:2882–2890.
5. Bruggeman LA, O'Toole JF, Sedor JR (2017) Identifying the intracellular function of APOL1. *J Am Soc Nephrol* 28:1008–1011.
6. Schmidtke G, Aichem A, Groettrup M (2014) FAT10ylation as a signal for proteasomal degradation. *Biochim Biophys Acta* 1843:97–102.
7. Basler M, Buerger S, Groettrup M (2015) The ubiquitin-like modifier FAT10 in antigen processing and antimicrobial defense. *Mol Immunol* 68:129–132.
8. Hipp MS, Kalveram B, Raasi S, Groettrup M, Schmidtke G (2005) FAT10, a ubiquitin-independent signal for proteasomal degradation. *Mol Cell Biol* 25:3483–3491.
9. Fan Y, et al. (2014) Temporal profile of the renal transcriptome of HIV-1 transgenic mice during disease progression. *PLoS One* 9:e93019.
10. Sampson MG, et al.; Nephrotic Syndrome Study Network (2016) Integrative genomics identifies novel associations with APOL1 risk genotypes in black NEPTUNE subjects. *J Am Soc Nephrol* 27:814–823.
11. Pasaniuc B, et al. (2011) Enhanced statistical tests for GWAS in admixed populations: Assessment using African Americans from CARe and a breast cancer consortium. *PLoS Genet* 7:e1001371.
12. Maples BK, Gravel S, Kenny EE, Bustamante CD (2013) RFMix: A discriminative modeling approach for rapid and robust local-ancestry inference. *Am J Hum Genet* 93:278–288.
13. Price AL, et al. (2009) Sensitive detection of chromosomal segments of distinct ancestry in admixed populations. *PLoS Genet* 5:e1000519.
14. Auton A, et al.; 1000 Genomes Project Consortium (2015) A global reference for human genetic variation. *Nature* 526:68–74.
15. International HapMap Consortium (2005) A haplotype map of the human genome. *Nature* 437:1299–1320.
16. Patterson N, et al. (2004) Methods for high-density admixture mapping of disease genes. *Am J Hum Genet* 74:979–1000.
17. Freedman ML, et al. (2006) Admixture mapping identifies 8q24 as a prostate cancer risk locus in African-American men. *Proc Natl Acad Sci USA* 103:14068–14073.
18. Genovese G, Friedman DJ, Pollak MR (2013) APOL1 variants and kidney disease in people of recent African ancestry. *Nat Rev Nephrol* 9:240–244.
19. Visscher PM, et al. (2017) 10 years of GWAS discovery: Biology, function, and translation. *Am J Hum Genet* 101:5–22.
20. Edwards SL, Beesley J, French JD, Dunning AM (2013) Beyond GWASs: Illuminating the dark road from association to function. *Am J Hum Genet* 93:779–797.
21. Lappalainen T, et al.; Geuvadis Consortium (2013) Transcriptome and genome sequencing uncovers functional variation in humans. *Nature* 501:506–511.
22. Patterson N, Price AL, Reich D (2006) Population structure and eigenanalysis. *PLoS Genet* 2:e190.
23. Stegle O, Parts L, Durbin R, Winn J (2010) A Bayesian framework to account for complex non-genetic factors in gene expression levels greatly increases power in eQTL studies. *PLOS Comput Biol* 6:e1000770.
24. Nichols B, et al. (2015) Innate immunity pathways regulate the nephropathy gene Apolipoprotein L1. *Kidney Int* 87:332–342.
25. Gong P, et al. (2010) The ubiquitin-like protein FAT10 mediates NF-kappaB activation. *J Am Soc Nephrol* 21:316–326.
26. Olabisi OA, et al. (2016) APOL1 kidney disease risk variants cause cytotoxicity by depleting cellular potassium and inducing stress-activated protein kinases. *Proc Natl Acad Sci USA* 113:830–837.
27. Canaan A, et al. (2006) FAT10/diubiquitin-like protein-deficient mice exhibit minimal phenotypic differences. *Mol Cell Biol* 26:5180–5189.
28. Raasi S, Schmidtke G, Groettrup M (2001) The ubiquitin-like protein FAT10 forms covalent conjugates and induces apoptosis. *J Biol Chem* 276:35334–35343.
29. Snyder A, et al. (2009) FAT10: A novel mediator of Vpr-induced apoptosis in human immunodeficiency virus-associated nephropathy. *J Virol* 83:11983–11988.
30. Merbl Y, Refour P, Patel H, Springer M, Kirschner MW (2013) Profiling of ubiquitin-like modifications reveals features of mitotic control. *Cell* 152:1160–1172.
31. Barton NH (2000) Genetic hitchhiking. *Philos Trans R Soc Lond B Biol Sci* 355:1553–1562.
32. Beckerman P, et al. (2017) Transgenic expression of human APOL1 risk variants in podocytes induces kidney disease in mice. *Nat Med* 23:429–438.
33. Kozlitina J, et al. (2016) Plasma levels of risk-variant APOL1 do not associate with renal disease in a population-based cohort. *J Am Soc Nephrol* 27:3204–3219.
34. Ross MJ, et al. (2006) Role of ubiquitin-like protein FAT10 in epithelial apoptosis in renal disease. *J Am Soc Nephrol* 17:996–1004.
35. Kalveram B, Schmidtke G, Groettrup M (2008) The ubiquitin-like modifier FAT10 interacts with HDAC6 and localizes to aggresomes under proteasome inhibition. *J Cell Sci* 121:4079–4088.